J. Materials, Conc. Struct. Pavements, JSCE, No. 697/V-54, 215-225, 2002 February

CONCEPTS OF LOCALIZED COMPRESSIVE FAILURE OF CONCRETE IN RC DEEP BEAMS

Torsak LERTSRISAKULRAT[1], Junichiro NIWA[2], Akinori YANAGAWA[3] and Maki MATSUO[4]

[1]Member of JSCE, Ms. Eng., Graduate Student, Dept. of Civil Eng., Tokyo Institute of Technology (2-12-1 O-okayama, Meguro-ku, Tokyo 152-8552, Japan)
[2]Fellow of JSCE, Dr. Eng., Professor, Dept. of Civil Eng., Tokyo Institute of Technology
[3]Undergraduate Student, Dept. of Civil Eng., Tokyo Institute of Technology
[4]Member of JSCE, Ms. Eng., Research Associate, Dept. of Civil Eng., Tokyo Institute of Technology

RC deep beams with the effective depth of 200, 400 and 600 mm and with the transverse reinforcement ratio varied from 0.0, 0.4 to 0.8 percent are tested. The measurement on the distribution of the local strains inside specimens for both concrete and reinforcements is performed by embedded strain gages inside the deep beams. The localized compressive failure zone of concrete in RC deep beams, which failed in shear compressive mode, is identified. Thus, the localized failure volume, V_p, and the fracture energy, G_{Fc}, are quantitatively evaluated. It is proved that concepts of G_{Fc} from the uniaxial compression tests are also applicable to concrete in RC deep beams which locally fail in compression.

Key Words : *RC deep beams, localized compressive failure, fracture energy in compression, localized compressive failure volume*

1. INTRODUCTION

Recently, it has been recognized that failure of concrete in compression is a localized phenomenon[1)-5)]. As a result, the descending path of the stress-strain curve is size-dependent and cannot be considered as material property. Several attempts have been conducted for measuring the local strain inside concrete specimens subjected to uniaxial compressive load[3)-5)], but none to the beam tests [6)]. Hence, the localized compressive failure of concrete in reinforced concrete (RC) beams remains unsolved and need to be clarified.

One remarkable and interesting example of the compressive failure of concrete in RC beams is the RC deep beams failed in shear compression. Deep beams are structural elements having a shear span to effective depth ratio, a/d, not exceeding 1. Due to the geometry of deep beams, they behave as two-dimensional members, rather than one-dimensional, subjected to a two-dimensional state of stress. As a result, plane cross-sections before bending could not necessarily remain plane after bending. The resulting strain distribution can be no longer considered as linear, and shear deformations that are normally neglected in slender beams become significant. Moreover, the significant parameter of the RC deep beams which should be taken into account is the shear resisting mechanism, as the diagonal cracks that develop in the beams are considerably wider than the flexural cracks and the abrupt failure without advanced warning is distinctly different from the failure in flexure.

In addition, at the final failure state of RC deep beams, the compressive failure along the compressive arch connecting between the loading point and support is usually observed, together with concrete crushing due to compression at the upper portion of the beams in the vicinity area under the loading point.

Therefore, investigation on compressive shear failure behavior is conducted on series of deep beams with the effective depth equal to 200, 400 and 600 mm subjected to the concentrated load at the mid span, based on the techniques of local strain measurement by Nakamura and Higai[3)]. The effects

Table 1 Outlines of the experiments

Specimen	r_w (%)	Stirrups (SD295A)	Deformed PC bars	Top bars (SR235)	d (mm)	h (mm)	2a (mm)	L (mm)	r (mm)
D200	0.00	None	PC-ϕ 19	ϕ 6	200	250	400	1,000	50
D204	0.42	D6@100							
D208	0.84	D6@50							
D400	0.00	None	PC-ϕ 25	ϕ 6	400	450	800	1,400	100
D404	0.42	D6@100							
D408	0.84	D6@50							
D600	0.00	None	PC-ϕ 32	ϕ 6	600	650	1,200	1,800	150
D604	0.42	D6@100							
D608	0.84	D6@50							

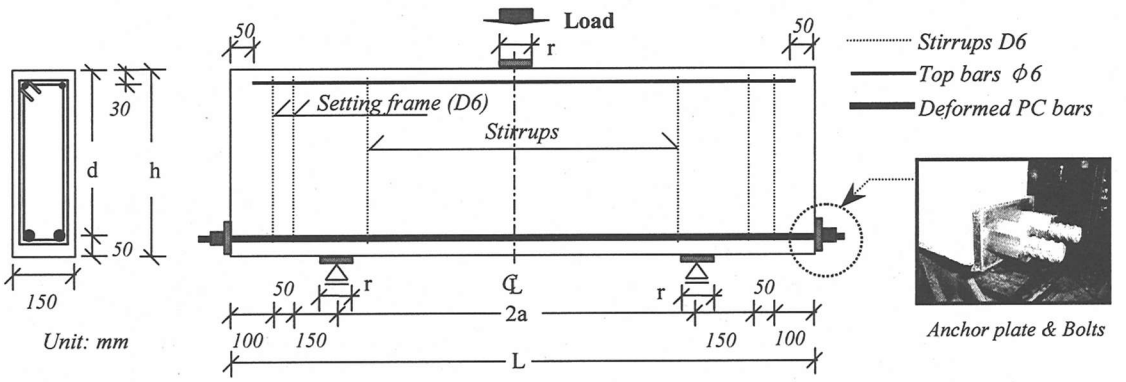

Fig. 1 Schematic drawing of the RC deep beam specimen

of the transverse reinforcement on the localized compressive behavior are also studied. Subsequently, the localized failure volume and the fracture energy of the concrete which fails in compression in RC deep beams are evaluated. The obtained concrete fracture energy in compression from the RC deep beam tests is compared with that of the uniaxial compression tests[5].

2. BACKGROUND OF THE RESEARCH

RC deep beams are widely used in the construction, such as tall buildings, offshore structures and complex foundation systems. The strength of RC deep beams is usually controlled by shear rather than flexure when a normal amount of longitudinal reinforcement is provided. An understanding of the shear resisting mechanism of RC deep beams is an essential prerequisite for achieving the optimum design and proportioning of the members.

The shear action in RC deep beams leads to compression in a diagonal direction and tension in a direction perpendicular thereto. For a deep beam in which the end anchorage of the longitudinal reinforcement is carefully designed, the possible failure mode is the web compression failure (crushing of concrete).

On the other hand, it has been found, recently, that not only the concrete fails in tension but also the concrete fails in compression, showing the significant localized failure phenomenon[1)-5)]. This means the size effect exists in the concrete failed under compression. In the uniaxial compression tests, such parameters of localized compressive failure as localized failure volume and the compressive fracture energy have been proposed[3)-5)]. Therefore, if the localized compressive failure of concrete along the compressive arch in RC deep beams, which failed in shear compression mode, can be confirmed, this might be able to explain why the size effect in RC deep beams exists. In addition, it is interesting to find out the parameters of localized compressive failure also for the concrete in RC deep beams with and without the transverse reinforcement and compare with those from the uniaxial compression tests[5].

3. EXPERIMENTS OF RC DEEP BEAMS

(1) Outlines of the experiments

Figure 1 shows the schematic diagram of the deep

Table 2 Mixing proportion and mechanical properties of reinforcements

(a) Mixing proportion

W/C (%)	*s/a* (%)	Unit content (kg/m^3)			
		W	*C*	*S*	*G*
50	49	190	380	853	898

C:high early strength portland cement; S:river sand; G:crushed stone, max. size=13mm; age of test 7 days (excepts D404, 49 days); air content 2.5%; no water reducing agent or superplasticizer.

(b) Mechanical properties of reinforcements

Reinforcement	Size/Grade	Area (mm^2)	E_s (N/mm^2)	f_y (N/mm^2)	f_u (N/mm^2)
Top bar	ϕ6/SR235	28.27	2.00×10^5	310	452
Vertical steel	D6/SD295A	31.67	2.00×10^5	331	509
Deformed PC bar (Type B)	PC-ϕ19	286.50	2.01×10^5	1,026	1,127
	PC-ϕ25	506.70	2.00×10^5	1,004	1,130
	PC-ϕ32	794.20	2.01×10^5	1,006	1,147

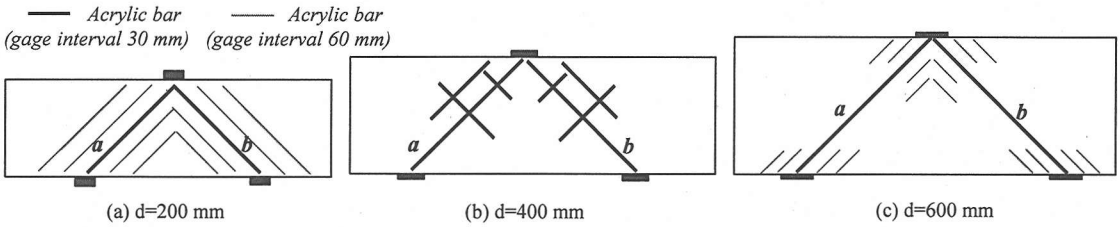

(a) d=200 mm (b) d=400 mm (c) d=600 mm

Fig. 2 Arrangement of the deformed acrylic bars (All strain gages were aligned parallel to the directions of the compressive arch on each side (direction of acrylic bars *a* and *b*))

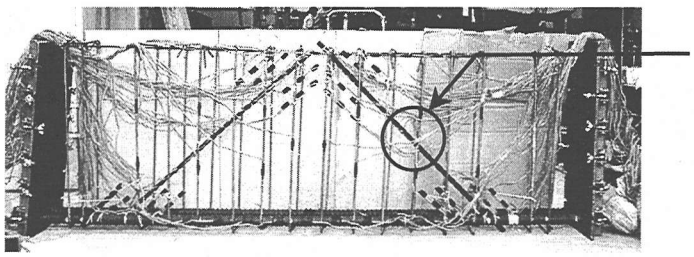

Deformed acrylic bar (attached by strain gages)

(a) Specimen before casting

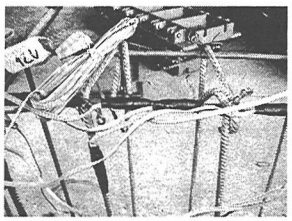

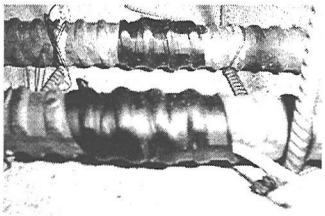

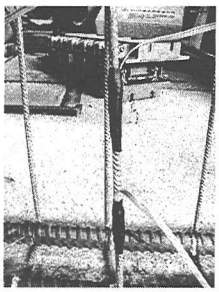

Top bar Deformed PC bar Stirrup

(b) Strain gages attached to the reinforcements

Fig. 3 Preparation of the specimen

beam specimen in the tests. The loading span, 2a, is varied as 400, 800 and 1200 mm, for the effective depth, d, of 200, 400 and 600 mm, respectively, so that a/d ratio is equal to 1 in all cases. The overall length, L, is 600 mm longer than the loading span in all cases. All beams are 150-mm wide and the thickness of cover concrete from the center of the PC bars to the tensile face of all beams is 50 mm. For the beams with the same effective depth, d, the transverse reinforcement ratio, r_w, is varied from 0.00, 0.42 to 0.84 percent. The ratio of the loading plate width, r, to the effective depth, d, is maintained to be 0.25, i.e. r/d=0.25, for all cases.

Details of the dimension and reinforcements of specimens are tabulated in **Table 1**. The beams were cast with the concrete mixed with the maximum aggregate size of 13 mm and reinforced by deformed PC bars as tensile reinforcement. The mixing proportion of concrete and mechanical properties of reinforcements are summarized in **Table 2(a)** and

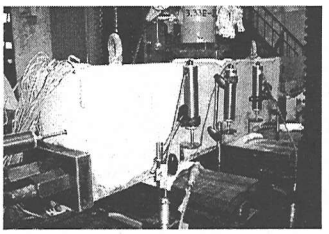

(a) Set up of specimen before testing

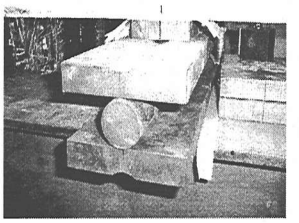

(b) Support

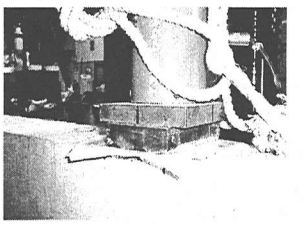

(c) Load cell

Fig. 4 Test set up

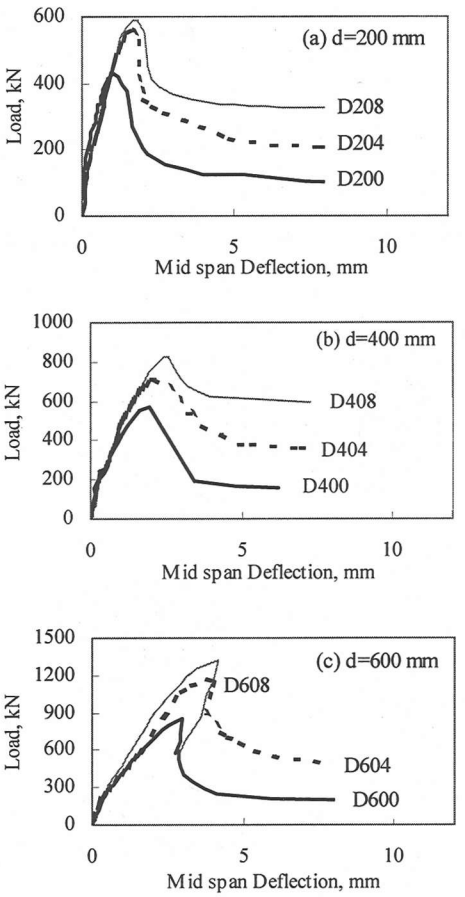

Fig. 5 Load- mid span deflection curves of the tested beams

(b). It is noted that the anchor plates and bolts are employed at both ends of the beam in order to ensure the sufficient anchorage between concrete and deformed PC bars.

The crucial point of this study is to measure local strains of concrete inside the beams by embedded deformed acrylic bars attached by strain gages with the interval of either 30 or 60 mm inside each specimen as depicted in **Figs. 2(a)** to **(c)**. The reliability of the results measured applying this technique had been verified by comparing the externally measured deformation (using deflection gages) with the summation of that locally measured by internal strain gages[5]. The strain gages were also attached to the reinforcements, i.e. top bars, bottom bars (deformed PC bars) and stirrups, in addition to the acrylic bars. The locations of deformed acrylic bars and the preparation of specimens before casting are illustrated in **Fig. 3(a)** and **(b)**.

Figure 4(a) to **(c)** show the experimental set up of a specimen and the equipment. The beam was placed over the roller support sets at the distance of 300 mm from each end. The support set, as shown in **Fig. 4 (b)**, was composed of the bearing plate, width r (**Table 1**), and 28-mm thick, over a set of two steel plates and a steel bar acting as a roller. A set of teflon sheets inserted with silicon grease was put between each bearing plate and the specimen in order to reduce the friction at the interface between the specimen and supports and to ensure the horizontal movement of the specimen during the test.

All beams were subjected to the concentrated load at the mid span through the loading plate. Deflection gages were installed at both faces of the mid span and over the both supports, and at the level of tensile reinforcement to measure the mid span deflection of the beam. An additional deflection gage was also installed horizontally at either end of a specimen to measure the horizontal movement of the beam.

Initiation and propagation of cracks have been visually detected while the specimens were loaded. In the post-peak region of the load-mid span deflection curve, the one-directional repeated loading technique was utilized, in order that the complete descending path of the load-deflection curve could be captured.

(2) Experimental results

a) External measurement

The test results in **Figs. 5(a)** to **(c)** show load-mid span deflection curves of the beams with the same effective depth but different ratio of transverse

Table 3 Test results*

Specimen	P_{1st} (kN)	P_{sh} (kN)	P_{cr} (kN)	P_{max} (kN)	f'_c (N/mm^2)	f_t (N/mm^2)
D200	125.6	157.0	304.1	428.3	38.4	3.4
D204	107.9	215.8	-**	559.5	43.2	2.7
D208	104.0	145.2	578.8	591.4	34.2	3.1
D400	127.5	181.5	515.0	570.6	35.5	3.0
D404	137.3	235.4	627.8	711.8	27.5	2.8
D408	196.2	274.7	735.8	827.9	38.4	3.4
D600	215.8	245.3	588.6	848.9	40.8	2.4
D604	206.0	284.5	-**	1,173.3	34.2	3.1
D608	299.2	377.7	1,314.5	1,327.6	35.3	3.1

** The fracture energy of concrete in tension, G_F, is 0.16 N/mm for all cases.*
*** Results not available.*

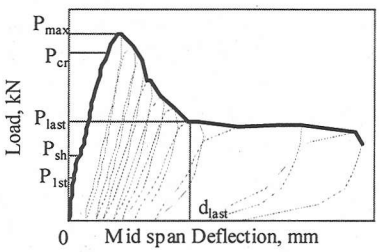

Fig. 6 Typical test results

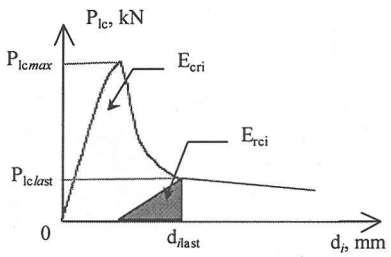

Fig. 7 Calculation of E_{cri}

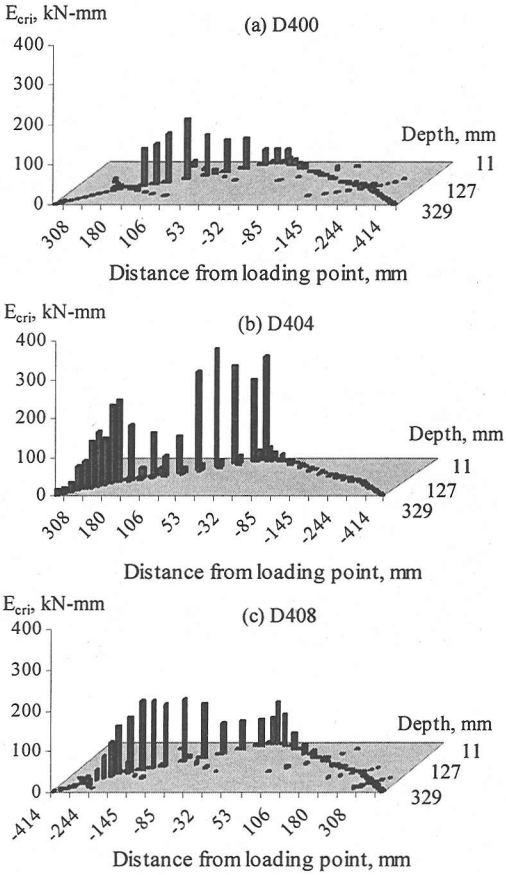

Fig. 8 Distribution of E_{cri} (d=400 mm series)

reinforcement. Concerning an actual path, a typical load-mid span deflection curve is shown in **Fig. 6** while all the test results are summarized in **Table 3**. As expected, the increase in the maximum load was observed when either the transverse reinforcement or the effective depth of the beam was increased. The higher ductility behavior of the beam was also seen when the transverse reinforcement ratio was increased.

The area under the curves from **Figs. 5(a)** to **(c)** is applied to the calculation of the concrete fracture energy in compression discussed later in section 4.2.

b) Internal measurement

From the local strain measurement, the local displacement can be obtained by multiplying the measured local strain by the interval between each strain gage, i.e. 30 or 60 mm. Then, the energy consumed locally by concrete, E_{cri}, can be calculated from the area under the local load-displacement curve of each gage excluding the recoverable portion, E_{rci} (**Fig. 7**). The calculation is made up to the point in which the gradient of the descending path of the load-mid span deflection curve started to become flat, namely up to the case where the mid span deflection, d_{last} (corresponding to P_{last}), was equal to 4, 6 and 10 mm for the cases of d=200, 400 and 600 mm, respectively.

Here, the local load, P_{lc}, was estimated from the simple strut-and-tie model as,

$$P_{lc} = P/(2\sin 45°) \qquad (1)$$

The local strain measured from the gages embedded inside the beam in case of D404, are given in **APPENDIX A**.

Distributions of E_{cri} in **Fig. 8(a)** to **(c)** (d=400 mm series) show that particular portions of concrete absorbed most of the energy while other portions absorbed very small or almost zero amount of energy. This means, when a deep beam failed in shear compression, the localization in compression occurred along the compressive arch, which connecting between the point of load application and supports. Consequently, determination of the localized compressive failure volume of the concrete in RC deep beams is discussed later in section 4.1.

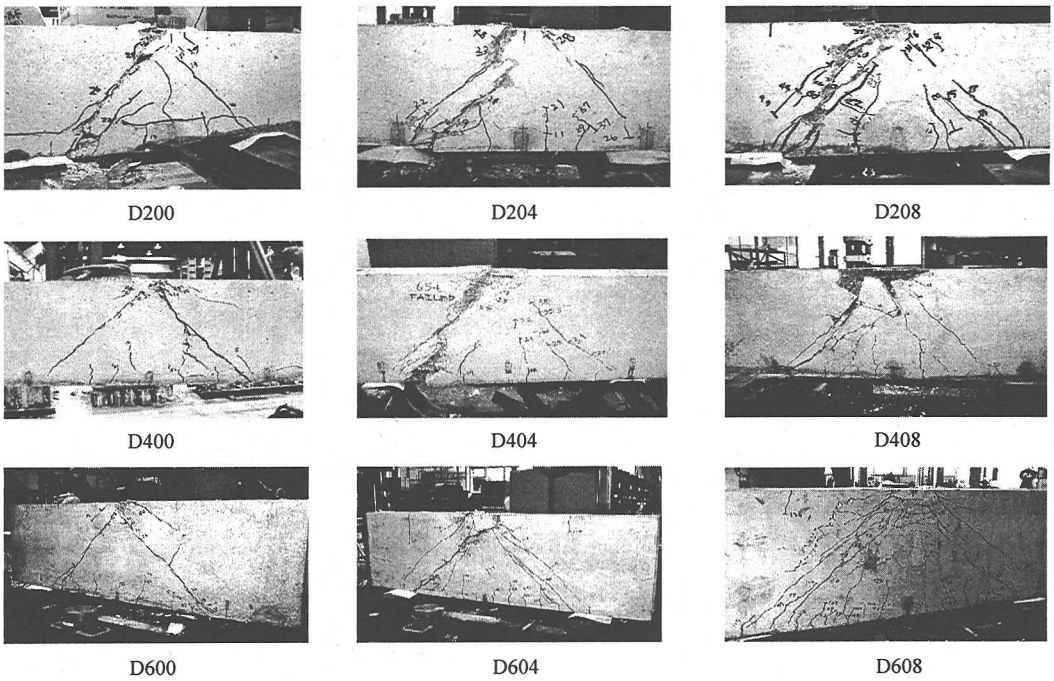

Fig. 9 Final failure of the specimens

It should be noted that, PC bars were employed as tensile reinforcement in order to ensure the compressive shear failure mode of the beams. Moreover, it was observed from the test results of the strain gages attached to the reinforcements that the maximum strains of the PC bars were far below the yielding limit in all cases, while some parts of the top bars and stirrups yielded in all cases of the beam with transverse reinforcement (**Fig. A2(a)**, **APPENDIX A**).

(3) Failure of the deep beams

From the observation during the tests, it was found that a few fine visible vertical flexural cracks at the bottom zone of the mid span were first observed when the first cracking load, P_{1st}, was reached. Then, at P_{sh}, a few inclined shear cracks suddenly developed and propagated along the directions of the compressive arch, which connecting between the supports and the point of loading. It resulted in the sudden change of the slope of the load-mid span deflection curve as demonstrated by the typical curve in **Fig. 6**.

When the beam was further loaded, the amount of both the diagonal (shear) cracks and the flexural cracks increased and the small cracks coalesced forming large cracks. At the high load level before the maximum load, P_{max}, was reached, the crushing of concrete in the vicinity of the loading point began at the crushing load, P_{cr}. After the peak load was reached, loading was still applied to the beam to capture the descending path of the load-mid span deflection curve until the gradient of its became horizontally flat. At the final stage, loading was maintained for a while to ensure the increase in the deflection of the beam, without the decrease of (or with a slightly change in) loading magnitude (i.e. the curve remained almost horizontal). During this period, in which the excessive deflection was applied to the beam, the occurrence of the secondary cracks was observed as shown in **Fig. 9**. However, it should be noted that all beams failed in shear compression mode (except D608), with compression failure of concrete along compression arch. This is why the calculation of energy is made up to d_{last} in order to eliminate the effect of the energy consumed by the secondary cracks from the compression failure. In addition, the symmetrical failure of diagonal cracks along the compressive arch at both sides of the beam was not observed. This is because a RC beam is non-homogeneous and the strength of the concrete throughout the specimen is distributed randomly. The severe failure generally took place only at one side of the beam.

Nevertheless, only in case of D608 the failure of fan-liked shape took place in the vicinity of loading point at the upper portion of the beam. Thus the failure of the beam occurred even though the overall load-mid span deflection did not show the softening of the descending path (**Fig. 5(c)**).

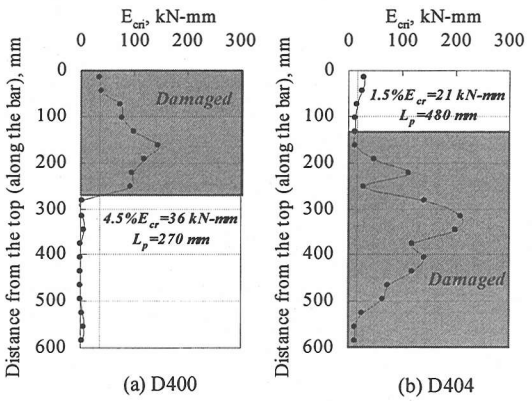

Fig. 10 Determination of failure zone

In addition, for beams with the same effective depth, the larger amount of cracks was observed when the transverse reinforcement ratio was increased.

4. PARAMETERS OF THE LOCALIZED COMPRESSIVE FAILURE

(1) Localized compressive failure volume, V_p

As shown in **Fig. 8**, the localized compressive failure zone can be quantitatively estimated from the calculated E_{cri}. From the external load-local strain distribution along the compressive arch, it was found that the failure always concentrated on one side of shear spans, while another side showed unloading behavior (see also **APPENDIX A**). Due to this reason, for the beam without transverse reinforcement (r_w=0.00%), the failure portion can be judged from the portion where E_{cri} is larger than 4.5 % of the summation of E_{cri} of all gages along the direction of the failure side of the compressive arch (i.e. either acrylic bar *a* or *b*, **Figs. 2(a)** to **(c)**), E_{cr}. On the other hand, for the beam with transverse reinforcement (r_w=0.42 and 0.84%) the criterion of 1.5 % was used. The determination of the failure zone is illustrated in **Figs. 10(a)** and **(b)** for the beam without and with transverse reinforcement, respectively. The criteria of 4.5 and 1.5 percent are empirically selected based on the comparison of the evaluated results with the actual failure region of the specimens from the tests, in accordance with the consideration on the shape of the external load-local strain distribution curves. However, it should be noted that, unlike the concrete tested under uniaxial compressive load in which the end friction can be removed[3)-5)], in deep beam tests, the effects of the friction between the loading plate and the specimen

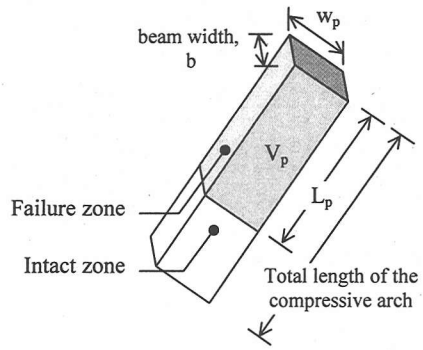

Fig. 11 Schematic figure of localized failure volume, V_p

would unavoidably happen. Hence, in order to distinguish between the failure zone and the intact zone, the consideration on only the magnitude of E_{cri} is insufficient because the shape of the load-local strain curves themselves is important. For example, from the results measured by the local strain gages located near the loading point, the concrete was subjected to high strain without showing the softening behavior of the unloading curves (see gage A1 and B1 of **Fig. A3, APPENDIX A**), that means concrete at the portion cracked but not failed, which is supposed to be due to the effects of the friction between the loading plate and specimen. In this case, the magnitude of E_{cri} was relatively high, but the concrete there was not judged to be failed.

Considering the shape of the load-local strain curves, the length of the localized compressive failure, L_p, has been determined. Then, the volume of the localized compressive failure, V_p, can be obtained as a result of L_p multiplied by the width of the compressive arch, w_p, and the width of the beam (150 mm) as depicted in **Fig. 11**. Here, the width of compressive arch, w_p, was taken from the previous research by Niwa[7)], which is calculated from the summation of the width of the bearing plate, r, and the 0.3 times the effective depth of the beam, multiplying by sin45°, as shown in Eq.(2).

$$w_p = (r + 0.3d) \times \sin 45° \qquad (2)$$

The results of L_p, w_p and V_p are summarized in **Table 4**. It is noted that, for D608, the failure pattern of the beam was different from the other cases. The failure of fan-liked shape was observed. Therefore, L_p was obtained from both sides of the compressive arch, while E_{cr} was the summation of the E_{cri} of the gages along both the deformed acrylic bars *a* and *b*.

Figure 12 shows the value of V_p obtained from the experiment. The increase in V_p was observed when the transverse reinforcement ratio was increased. However, in cases of d=200 mm, the constant value of V_p was observed, in other words, the failure

Table 4 Localized failure volume (V_p) and compressive fracture energy of concrete (G_{Fc})

Specimen	L_p (mm)	w_p (mm)	V_p ($\times 10^6$ mm^3)	E_{ext} (kN-mm)	E_{yield} (kN-mm)	K_1 (%)	E_{net} (kN-mm)	G_{Fc} (N/mm^2)	G'^{**}_{Fc} (N/mm^2)	$\frac{G_{Fc}}{G'_{Fc}}$
D200	300	78	3.50	891	0	90	802	0.229	0.214	1.07
D204	300	78	3.50	1,265	13	85	1,064	0.304	0.220	1.38
D208	300	78	3.50	1,458	46	93	1,313	0.375	0.208	1.80
D400	270	156	6.30	1,614	0	87	1,404	0.223	0.210	1.06
D404	480	156	11.20	2,527	20	89	2,231	0.199	0.197	1.01
D408	420	156	9.80	3,238	494	81	2,223	0.227	0.214	1.06
D600	405	233	14.18	2,725	0	89	2,425	0.171	0.217	0.79
D604	540	233	18.90	5,528	578	78	3,861	0.204	0.208	0.98
D608	600	233	21.00	5,930*	-	89	5,278	0.251	0.210	1.20

** E_{ext} of D608 was estimated from the internal measurement using acrylic bars.*
*** G'_{Fc} is the compressive fracture energy from the uniaxial compressive tests (Eq. (6)).*

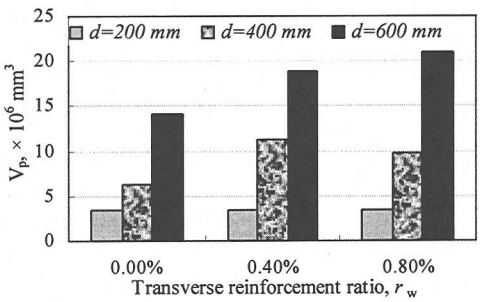

Fig. 12 Localized compressive failure volume, V_p

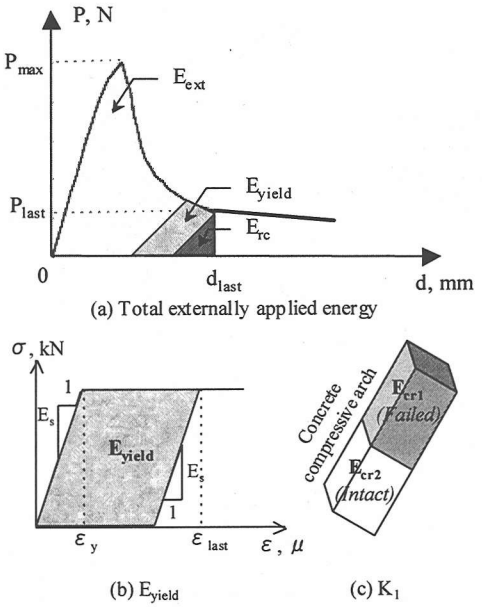

Fig. 13 Calculation of externally applied energy consumed by the localized compressive failure zone, E_{net}

occurred throughout the compressive arch in all the cases. This means the localized compressive failure of concrete did not take place for RC deep beams with d=200 mm.

(2) Compressive fracture energy, G_{Fc}

The fracture energy of concrete, which failed in compression, G_{Fc}, is computed based on the obtained V_p and the externally applied energy that caused localized compressive failure to concrete, E_{net}. Because G_{Fc} is defined as the energy required to cause compressive failure to a unit volume of concrete, effects of confinement from the stirrups or of the friction between the loading plate and specimen, which consumed some parts of externally applied energy, should be taken into account properly.

Hence, for beams without transverse reinforcement, at the first step, E_{ext} is calculated from the area under load-mid span deflection curve, excluding the part that can be recovered when unloaded, E_{rc} (the same concept as E_{cri} and E_{rci}, see **Fig. 13(a)**). Then, E_{net} is obtained by multiplying E_{ext} by the localized factor, K_1, which is the ratio of the summation of the local energy, E_{cri}, consumed by the failure portion to the total local energy consumed along the compressive arch (**Fig. 13(c)**), as shown in Eq. (3). The factor K_1 has been introduced in order to take into account the fraction of the externally applied energy which was consumed by the friction force (or also from the effects of the confinement from the stirrups in case of specimens with transverse reinforcement). It was found that the value of K_1 is in the order of 80 to 90 %, as shown in **Table 4**.

$$K_1 = \frac{E_{cr1}}{E_{cr1} + E_{cr2}} \tag{3}$$

For beams with transverse reinforcement, the energy consumed by the yielded reinforcements, E_{yield}, was excluded from the E_{ext} before multiplying by K_1 as shown in Eq. (4). The calculation of E_{yield} based on measured local strains of the reinforcements, i.e. top bars or transverse reinforcements, and the bilinear, elastic-perfectly plastic model (**Fig. 13 (b)**).

$$E_{net} = K_1(E_{ext} - E_{yield}) \tag{4}$$

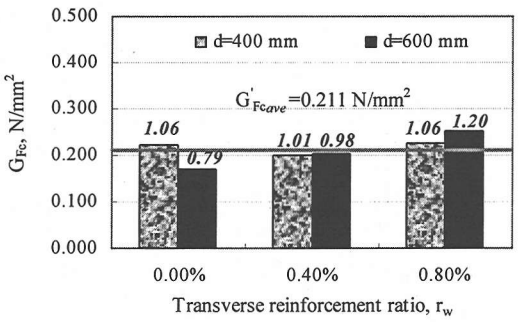

Fig. 14 Comparison of G_{Fc} from the beam tests and G'_{Fc} from the uniaxial compression tests

Then, G_{Fc} is determined by dividing the obtained E_{net} by V_p, as shown in Eq. (5). Results are summarized in **Table 4**.

$$G_{Fc} = E_{net} / V_p \quad (N/mm^2) \qquad (5)$$

In addition, the E_{ext} in case of D608 was estimated from the summation of E_{cri} of all the strain gages attached to the deformed acrylic bars within the failure zone. The results of G_{Fc} are summarized in **Table 4**.

5. COMPARISON OF G_{Fc}

Comparison between G_{Fc}, obtained from the deep beam tests, and G'_{Fc}, from the uniaxial compression tests, has been made. In the previous research[5], the experimental study on the localized compressive failure of the plain concrete with various cross-sectional size and shape, and also different cylindrical compressive strength, f'_c, subjected to uniaxial compressive stress was carried out. The local strain distributions inside concrete specimens subjected to externally applied load were measured, and the friction between the specimen and loading plates at each end of the specimen had been removed.

It was found that G'_{Fc} depends only on f'_c, and was proposed by the following Eq. (6).

$$G'_{Fc} = 0.86 \times 10^{-1} f_c'^{1/4} \quad (N/mm^2) \qquad (6)$$

The results of the comparison are plotted as shown in **Fig. 14**. The values denoted in the figure are the value of G_{Fc} and the comparison with G'_{Fc}, i.e. G_{Fc} / G'_{Fc}. Noted that the results of the cases as d=200 mm were not included because the localized compressive failure of concrete in the beams did not take place.

It is obvious that G_{Fc} values from RC deep beam tests agree well with those of the uniaxial compression tests when the energy consumed by the concrete was properly evaluated. This means the concept of localized compressive failure of concrete from the uniaxial compression tests can be applied to the concrete in RC deep beams as well. In other words, once a concrete member is subjected to the externally applied load, if the localized compressive failure occurs, the localized compressive failure volume depends on the externally applied energy which consumed by the concrete, in such a way that the externally applied energy per unit failure volume, i.e. G_{Fc}, becomes constant.

6. CONCLUSIONS

The localized compressive failure of the concrete in RC deep beams with and without transverse reinforcement are studied. In addition to the strain gages attached to the reinforcements, the strain gages were also attached to the deformed acrylic bars and embedded inside the beams in order to investigate the distributions of the local strain of concrete, especially, along the directions of the concrete compressive arch. Evaluation of the localized compressive failure volume, V_p, based on the shape of the load-local displacement curves and the energy consumed locally by concrete is proposed. The test results show that V_p is more or less increased with the increase in the transverse reinforcement ratio, r_w. Nevertheless, the constant value of V_p in the cases of d=200 mm indicated that the localized compressive failure did not occur.

Subsequently, the compressive fracture energy of concrete, G_{Fc}, is determined based on the obtained localized compressive failure volume and the externally applied energy that caused compressive failure to the concrete. The results show the almost constant value of G_{Fc} and also indicate good agreement between G_{Fc} obtained from RC deep beam tests and the uniaxial compression tests, when the externally applied energy is properly evaluated. For RC deep beams which fail in shear compression mode, the energy required to cause compressive failure to a unit volume of concrete is constant.

It can be concluded that RC deep beam is an evident example among the RC structures in which the concepts of the localized compressive failure of concrete is applicable, because of the obvious compressive stress flow directly from the point of loading to supports along compressive arch. Therefore, further studies on the localized compressive failure for the other types of RC structure having some parts fail in compression, are important.

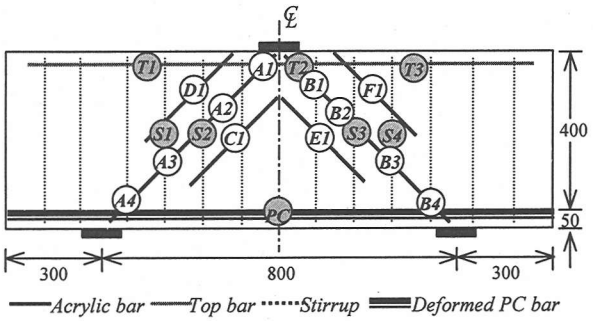

Fig. A1 Locations of local strain gages (D404)

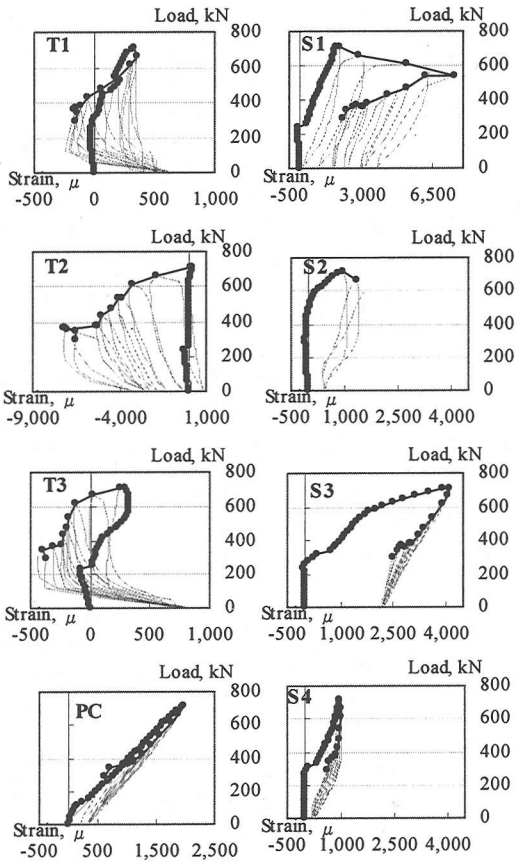

Fig. A2 Local strain distributions (D404: Reinforcement)

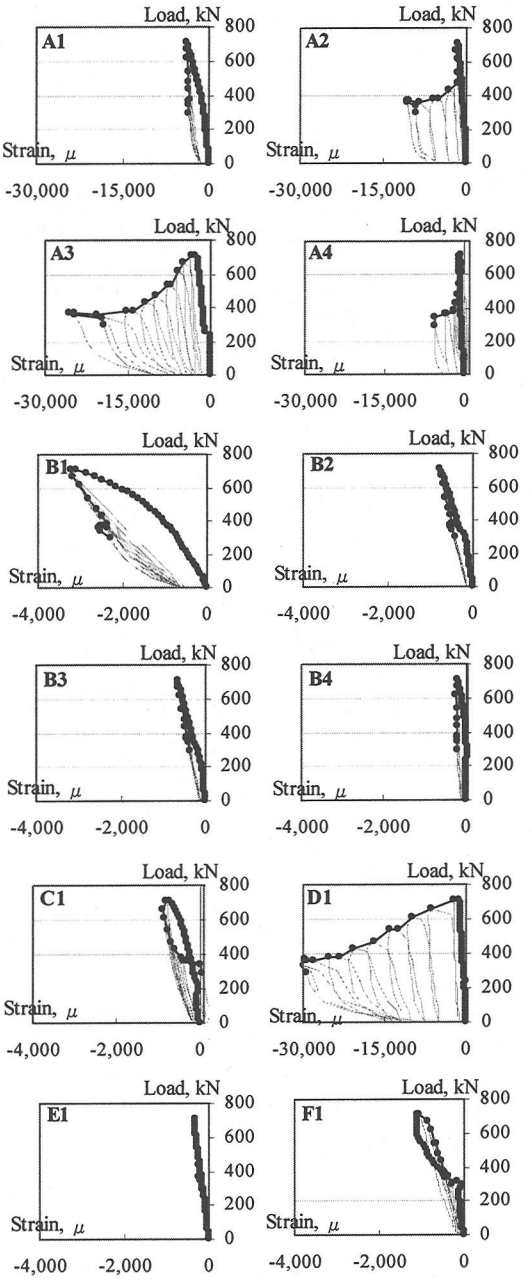

Fig. A3 Local strain distributions (D404: Concrete)

APPENDIX A LOCAL STRAINS INSIDE THE RC DEEP BEAMS

The samples of the test results are illustrated in this section. **Figure A1** depicts the diagram of the location of the internal strain gages, while the relationship between the external load-local strain of concrete and reinforcements are shown in **Figs. A2** and **3** (D404).

From the results of the strain gages attached to the deformed acrylic bars, it can be seen that the failure took place on the left hand side of the specimen (**Fig. A1**) as the softening curves were observed at some parts of acrylic bars, i.e. gages A2, A3, D1 in **Fig. A3**. Whereas the results of the other strain gages showed the unloading curves.

On the other hand, the results of the strain gages attached to the reinforcements showed that most of

reinforcements did not yield, except the gage T2 which was attached to the top bar at the location nearby the center line.

REFERENCES

1) Santiago, S.D. and Hilsdorf, H.K.: Fracture mechanisms of concrete under compressive loads, *Cement and Concrete Research*, Vol.3, pp. 363-388, 1973.
2) Markeset, G.: Failure of concrete under compressive strain gradients, *Dr.Eng thesis 1993:110,* Norwegian Institute of Technology, Trondheim, 1993.
3) Nakamura, H. and Higai, T.: Compressive fracture energy and fracture zone length of concrete, *JCI-C51E Seminar on Post-Peak Behavior of RC Structures Subjected to Seismic Loads*, Vol.2, pp. 259-272, Oct. 1999.
4) Lertsrisakulrat T., Watanabe K., Matsuo M. and Niwa J.: Localization Effects and Fracture Mechanics of Concrete in Compression, *Proceedings of the Japan Concrete Institute*, Vol.22, No.3, pp. 145-150, 2000.
5) Lertsrisakulrat, T., Watanabe K., Matsuo M. and Niwa J.: Experimental study on parameters in localization of concrete subjected to compression, *Journal of Materials, Concrete Structures and Pavements, JSCE*, No.669/V-50, pp.309-321, Feb. 2001.
6) Tan, K.H. and Lu, H.Y.: Shear behavior of large reinforced concrete deep beams and code comparisons, *ACI Structural Journal*, pp. 836-845, Sep.-Oct. 1999.
7) Niwa, J.: Equation for shear strength of reinforced concrete deep beams based on FEM analysis, *Concrete Library of JSCE*, No.4, pp. 283-295, Dec. 1984.

(Received March 1, 2001)

RCディープビームにおけるコンクリートの局所的圧縮破壊の考え方

Torsak LERTSRISAKULRAT・二羽淳一郎・柳川明哲・松尾真紀

有効高さ(d)を200，400，600(mm)，せん断補強筋比を0，0.4，0.8(%)としたRCディープビームのせん断破壊実験を行った．ディープビーム内部にひずみゲージを埋め込み，供試体内部のコンクリートと補強筋の局所ひずみ分布を測定した．せん断圧縮モードで破壊するRCディープビームにおけるコンクリートの局所的な圧縮破壊領域を定量的に把握し，最終的にコンクリートの破壊領域体積(V_p)と圧縮破壊エネルギー(G_{Fc})を決定した．そして，無補強コンクリートの一軸圧縮試験から得られたG_{Fc}の概念が，局所的な圧縮破壊を生じるディープビーム中のコンクリートにも同様に適用可能であることを示した．